ChemComm

A Double-Decker Cage for Allosteric Encapsulation of ATP

Journal:	*ChemComm*
Manuscript ID	CC-COM-02-2022-000927.R1
Article Type:	Communication

COMMUNICATION

A Double-Decker Cage for Allosteric Encapsulation of ATP

Han Xie,[a] Tyler J. Finnegan,[a] Vageesha W. Liyana Gunawardana,[a] William Xie,[a] Curtis E. Moore [a] and Jovica D. Badjić*[a]

Received 00th January 20xx,
Accepted 00th January 20xx

DOI: 10.1039/x0xx00000x

In this work, we describe the preparation of double-decker cage [1–H$_6$]$^{6+}$ comprising two binding pockets, each with three ammonium and three amide hydrogen bonding sites. This novel host possesses a high affinity for trapping two molecules of ATP in an allosteric fashion, with both experiments and theory suggesting the synergistic action of charged hydrogen bonds and π–π stacking in the encapsulation.

In living systems, adenosine-5'-triphosphate (ATP, Figure 1A) is the ubiquitous source of chemical energy.[1] The favorable hydrolysis of this compound drives a multitude of metabolic processes[2] including the propagation of electrical potential within nerves, intracellular signalling, muscle contraction, active transport of molecules across the cell wall and synthesis of biological compounds. Correspondingly, there has been a significant interest[3] toward developing abiotic receptors capable of selective detection,[4] visualisation,[5] and sequestration[6] of ATP as well as other nucleotides.[7] For instance, ATP is overexpressed in cancer cells wherein, among other things, it regulates the action of the P-glycoprotein molecular pump. This pump is embedded in the cell membrane to direct the active efflux of foreign molecules including anticancer drugs.[8] It has been suggested[6a] that sequestration of ATP within cancer cells could reduce drug resistance and improve the therapy. As ATP is a negatively charged molecule (i.e. α,β,γ–phosphates, Figure 1A) with a nonpolar aromatic group (i.e. adenine base, Figure 1A) the design of abiotic hosts has primarily centered on complementing these two sites via ion-ion,[4b] charged hydrogen bonds (HBs)[4a, 5b] and π–π stacking interactions.[4c, 9] To increase the effectiveness by which ATP is sequestered[10] but also build more effective chemosensors,[11] we reasoned that constructing hosts comprising two or more sets of binding sites could lead to the complexation of ATP in an allosteric fashion[5a, 12] with, potentially, each subsequent binding event being more exergonic than the prior one. Accordingly, we noted that hexasubstituted benzenes are sterically geared[13] to assume a stable *ababab* conformation in which 1,3,5 substituents point to one while 2,4,6 substituents to the opposite side of the benzene ring (Figure 1B). By connecting a set of these groups (e.g., 1-to-3-to-5, Figure 1B) with a complementary trivalent ligand, one can obtain a [1+1] tripodal cage with functional groups facing the inner space. Indeed, tripodal hosts of this kind have already been made[14] and studied for complexing gases,[15] carbohydrates,[16] and biologically relevant anions.[17] On the other side, a functionalization of both 1,3,5 and 2,4,6 groups with trivalent ligands gives a [1+2]

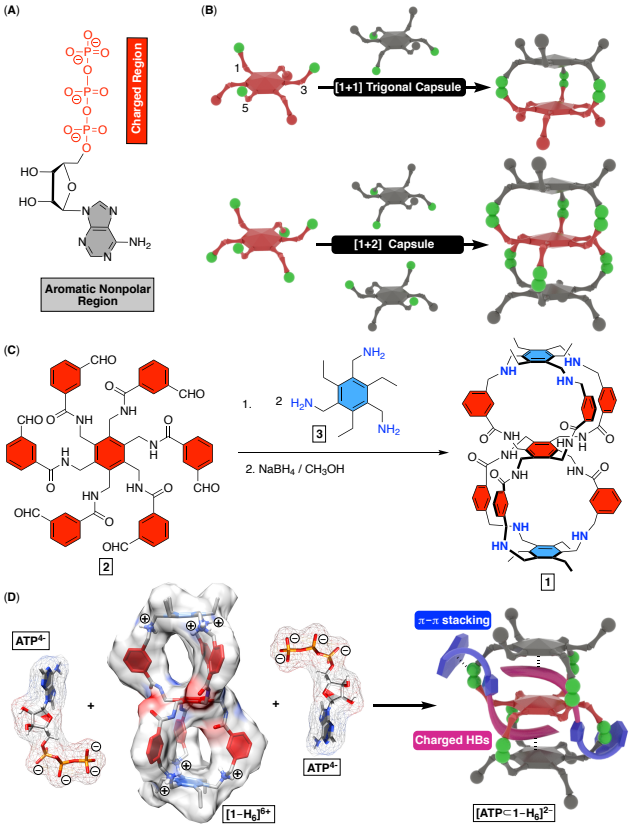

Figure 1. (A) Chemical structure of ATP^{4-}, with its polar and nonpolar regions targeted in the design of abiotic receptors. (B) A scheme showing the conformational preference of hexasubstituted benzenes, which is important for obtaining [1+1] and [1+2] tripodal cages. (C) The synthesis of double-decker cage **1**. (D) Energy-minimized conformers of [**1**-H$_6$]$^{6+}$ and two molecules of ATP^{4-} (MMFFs) reveal structural and electronic complementarity that could facilitate the formation of [ATP$_2$⊂**1**-H$_6$]$^{2+}$.

[a] *Department of Chemistry and Biochemistry, The Ohio State University, 100 West 18th Avenue, Columbus, OH (USA)*

Electronic Supplementary Information (ESI) available: Additional experimental and computational details. See DOI: 10.1039/x0xx00000x

tripodal cage with two adjacent cavities (Figure 1B).[18] It follows that previously studied[19] hexakis aldehyde **2** could undergo reversible imine condensations[20] with two molecules of *tris* amine **3** to, after a functional group transformation, give double-decker cage **1** (Figure 1C). This suggestion is also supported with recent studies[19, 21] in which we used templating anions to bias the conformation of hexakis aldehyde **2** for trapping a hexakis amine ligand giving a hexapodal capsule capable of binding anions in the kinetic fashion.[21] An energy-minimized conformer of [**1**–H_6]$^{6+}$ (MMFFs, Figure 1D) includes two adjoining pockets each with three ammonium and three amide sites. While these groups could hydrogen bond to triphosphates from ATPs, after their insertion into top and bottom cavities (Figure 1D), the aromatics from nonpolar belts might act in synergy to stabilize π surface of the nonpolar adenines. With this in mind, we set to prepare cage **1** and probe its capacity to trap nucleotides in an allosteric manner.[22]

Hexakis aldehyde **2** was synthesized by a previously published procedure[19] while 1,3,5-tris(aminomethyl)-2,4,6-triethyl-benzene **3** was obtained from 1,3,5-triethylbenzene.[23] After combining one equivalent of **2** with two equivalents of **3** in DMSO (Figure 1C), there followed a disappearance of the aldehyde singlet at 9.75 ppm (^{1}H NMR spectroscopy, Figure S4) with a concomitant emergence of RN=C–H resonance at 8.6 ppm to indicate the formation of desired imine cage. Indeed, high-resolution mass spectrometry (ESI) confirmed the presence of [1+2] product with *m*/*z* = 1457.7 (Figure S5). Due to the labile nature of the imine cage, we refrained from its isolation and decided to "fix" the imine bonds by hydride reduction (Figure 1C).[24] After adding an excess of $NaBH_4$ to the reaction mixture, ^{1}H NMR signal of the imine disappeared with the appearance of another set of resonances corresponding to **1**. Upon purification, [1+2] cage **1** was obtained in 26% yield with ^{1}H NMR spectrum (Figure 2B; see also Figure S1) corresponding to, on average, D_{3d} symmetric molecule. When **2**-to-**3** condensation was run in dimethylformamide (DMF, Scheme S1), the total yield of **1** increased to 40% (Table S1).

Vapor diffusion of diethyl ether into a solution of **1** in DMF resulted in the formation of single crystals. X-ray diffraction analysis revealed centrosymmetric **1** (Figure 2A) with two preorganized cavities, each lined with six positively polarized N–H$^{\delta+}$ groups pointing to the inner space. Three benzene rings comprising the floors and ceilings of double-decker **1** are nearly parallel and separated by 7.7 Å. Disordered molecules of DMF occupy the cage's interior by forming HBs with amine and amide N–Hs on the concave side. The notion that the synthesis of **1** was most effective in DMF (Table S1) goes well with the templating role of this solvent.[25]

To dissolve cage **1** in water and obtain a clear solution, we lowered the pH to 3 (HCl). Based on a literature precedent,[26] we deduced that **1** would at this pH have all of its amines protonated. Accordingly, standard solutions of [**1**–H_6]$^{6+}$ were made in 27 mM HEPES buffer at pH = 3 (Figure 2B) and then used to carry NMR binding studies described below. At pH = 3.0, ATP is predominantly a doubly charged anion with one proton at γ–phosphate and another at N–1 of the adenine base (pK_a(3) = 2.1, pK_a(4) = 4.0 and pK_a(5) = 6.5; Figure 3A).[27]

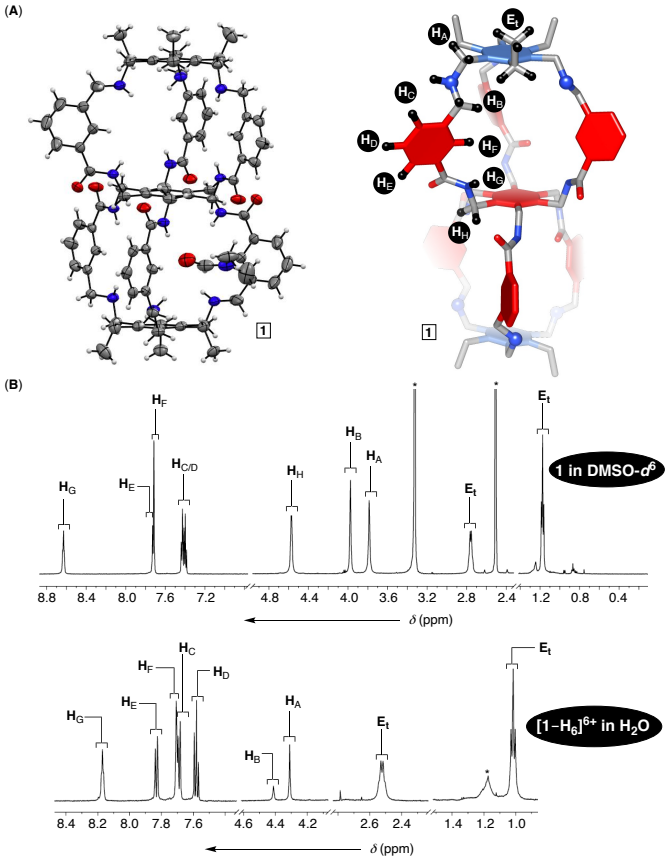

Figure 2. (A, top left) ORTEP diagram (50% probability) of double-decker cage **1**. ^{1}H NMR spectrum (700 MHz, DMSO-d^6) of **1** with its stick and ball representation (A, top right) showing the proton assignment. (B) Selected regions of ^{1}H NMR spectrum (700 MHz, H_2O) of [**1**–H_6]$^{6+}$ obtained after the solvent suppression (4.5 ppm).

An incremental addition of a standard solution of ATP^{2-} to [**1**–H_6]$^{6+}$ resulted in a steady movement of ^{1}H NMR resonances from both host and guest (Figure 3A; Figure S7). The intermolecular interaction was taking place fast on the chemical shift time scale with an excess of ATP^{2-} needed to saturate the host. Importantly, the proton nuclei from ATP^{2-} (**H**$_{1\text{-}3}$, Figure 3A) were magnetically shielded in the presence of [**1**–H_6]$^{6+}$. At the same time, benzene nuclei **H**$_{C/D/E}$ from [**1**–H_6]$^{6+}$ got shielded as well while the amide **H**$_G$ became deshielded with increased quantity of ATP^{2-}. With [**1**–H_6]$^{6+}$ lined with nine benzene rings, positioning a molecule of ATP^{2-} in its vicinity would result in an upfield shift of its resonances. If ATP^{2-} thus placed its phosphate inside the cavity of [**1**–H_6]$^{6+}$ (Figure 3A) then the observed downfield shift of the amide **H**$_G$ protons ought to be reporting on their hydrogen bonding with the phosphate. Provided the same scenario, the magnetic shielding of **H**$_{C/D/E}$ nuclei could have resulted from the adenine base stacking with the cage's benzene ring (Figure 3A). Indeed, ^{1}H-^{1}H NOESY spectrum of a solution containing 1.0 mM of [**1**–H_6]$^{6+}$ and 2.0 mM ATP^{2-} (Figure S8) showed cross peaks between adenine's **H**$_2$ and benzene's **H**$_{C/E}$ nuclei as well as ribose's **H**$_4$ and benzene's ***H***$_{C/D/E/F}$ nuclei (Figure 3A). That is to say, the experimental results are in line with the binding mode in which ATP^{2-} inserts its phosphate into a cavity of [**1**–H_6]$^{6+}$ while its adenine π–π stacks with benzene sides from, likely, another cavity (Figure 3A). By changing the proportion of [**1**-H_6]$^{6+}$ and ATP^{2-} and measuring the perturbation of ^{1}H NMR signals from the cage's **H**$_G$ and **H**$_E$ nuclei (Figure 3A), we constructed the Job plot peaking at ~0.33 to suggest

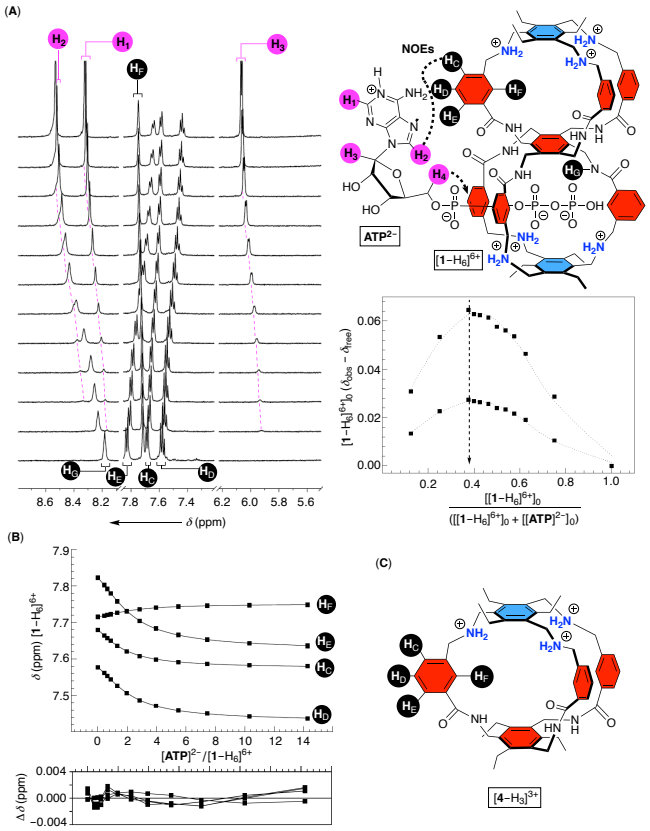

Figure 3. (A) Partial ^{1}H NMR spectra (700 MHz, 27 mM HEPES buffer at pH = 3.0) of 0.35 mM solution of [**1**–H$_6$]$^{6+}$ obtained upon an incremental addition of 23.3 mM standard solution of ATP^{2-} (0-14 molar equivalents). (Bottom right) The Job plot for the complexation of [**1**–H$_6$]$^{6+}$ by ATP^{2-} (total 1.0 mM) in 27 mM HEPES buffer at pH = 3.0 was obtained from ^{1}H NMR spectroscopic measurements. (B) The change in chemical shift (δ) of **H**$_{C/D/E/F}$ protons from [**1**–H$_6$]$^{6+}$ after incremental addition of ATP^{2-} (see A) would fit well to 1:2 complexation model (Figure S7) with a random distribution of residuals (bottom). (C) Chemical structure of [1+1] tripodal cage [**4**–H$_3$]$^{3+}$ (Scheme S1 and Figure

the formation of ternary [ATP$_2$⊂**1**–H$_6$]$^{2+}$. The nonlinear least-squares fit of ^{1}H NMR titration data to a 1:2 stoichiometric model was satisfactory (i.e., random residuals; Figure 3B)[28] with association constants $K_1 = 1.3 \pm 0.4 \cdot 10^4$ M^{-1} and $K_2 = 2.1 \pm 0.4 \cdot 10^3$ M^{-1} (Table 1). It follows that the formation of ternary [ATP$_2$⊂**1**–H$_6$]$^{2+}$ occurred with a negative cooperativity of two consecutive binding events ($\alpha = 4K_2/K_1 = 0.6$; for a statistical complexation $\alpha = 1$).[29] In the similar manner, we used ^{1}H NMR spectroscopy to probe the complexation of ADP$^-$ and AMP (Figures S9-S10)[30] thereby finding that the stability of the corresponding ternary and binary complexes would decrease

Table 1. Association constants K_1 and K_2 for the complexation of hosts [**1**-H$_6$]$^{6+}$ and [**4**–H$_3$]$^{3+}$ (last row) were obtained by nonlinear least-square analysis of experimental binding isotherms at 298 K (Figures S7/S9-12). The reported values are shown as a mean

Guest	K_1 (M^{-1})	K_2 (M^{-1})	$\alpha = 4K_2/K_1$
ATP^{2-}	$1.3 \pm 0.4 \cdot 10^4$	$2.1 \pm 0.4 \cdot 10^3$	0.6
ADP$^-$	$2.25 \pm 0.03 \cdot 10^2$	$7 \pm 3 \cdot 10^1$	1.2
AMP	–[a]	–[a]	–[a]
$H_2P_2O_7^{2-}$	$1.4 \pm 0.4 \cdot 10^3$	$3 \pm 2 \cdot 10^2$	0.9
ATP^{2-}[b]	$4.8 \pm 1.8 \cdot 10^2$	N.A.	N.A.

of three independent measurements ± standard deviation.

[a]No changes observed in ^{1}H NMR spectroscopic titration (Figure S10). [b]The complexation of [1+1] tripodal host [**4**–H$_3$]$^{3+}$ (Figure S12).

in the series of nucleotides (Table 1). The complexation of ADP$^-$ by [**1**–H$_6$]$^{6+}$ (Figure S9) caused similar magnetic perturbation of the cage's nuclei as ATP^{2-} (Figure 3A) indicating a comparable mode of association but noncooperative allostery ($\alpha = 1.2 \sim 1$, Table 1). On the other side, this less charged anion formed weaker electrostatic contacts with the hexacationic host.[4a] As AMP had no measurable affinity toward [**1**–H$_6$]$^{6+}$, we hypothesize that, apart its neutral charge, inserting a single phosphate sufficiently deep into the host would result in steric repulsions therefore inhibiting the interaction. And finally, pyrophosphate ($H_2P_2O_7^{2-}$, Table 1) having the same charge as ATP^{2-} at pH = 3 (pK_a(2) = 2.28 and pK_a(3) = 6.70) showed a weaker binding affinity toward [**1**–H$_6$]$^{6+}$ (Table 1) due to, we posit, the absence of aromatic adenine acting in synergy with the phosphate residue.[31] In this regard, [1+1] tripodal cage [**4**–H$_3$]$^{3+}$ (Figure 3C; Scheme S2), missing the "upper deck" and therefore a set of benzene rings for stabilizing ATP's adenine (Figure 3A), showed a comparable affinity toward ATP^{2-} as $H_2P_2O_7^{2-}$ toward [**1**–H$_6$]$^{6+}$ (use statistically corrected $K_1/2$ from $H_2P_2O_7^{2-}$ for comparison, Table 1). In support of the deduction, the complexation of ATP^{2-} caused greater magnetic perturbations of **H**$_{C/D/E/F}$ nuclei within stronger binding [**1**–H$_6$]$^{6+}$ (Figure 3B) than weaker binding [**4**–H$_3$]$^{3+}$ (Figure S12).

To further examine the nature of ternary complexes of ATP^{2-} and ADP$^-$ with [**1**–H$_6$]$^{6+}$, we completed replica exchange molecular dynamics (REMD) simulations.[32] In brief, REMD samples the conformational space more effectively than classical molecular dynamics (MD) by using a set of temperature baths for overcoming higher kinetic barriers corresponding to molecular movements

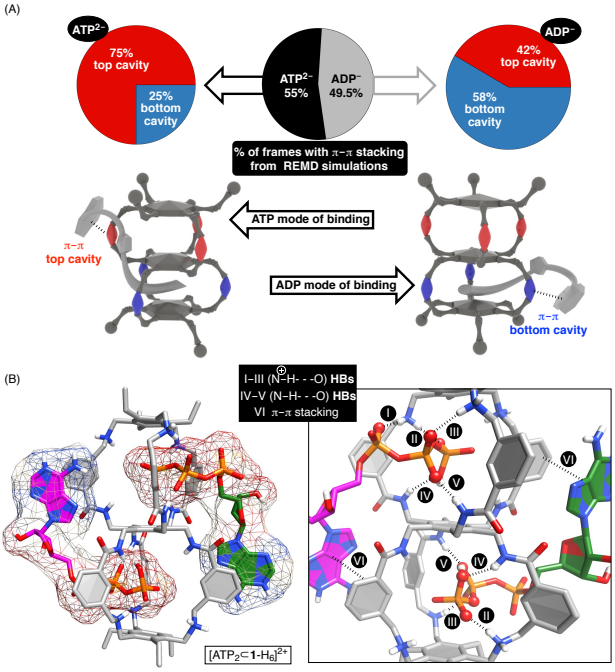

Figure 4. (A) Pie charts show percentage of time (or frames) that adenine base from ATP^{2-} and ADP$^-$ spends in the vicinity of benzene side arms (centroid-to-centroid distance of <4.5Å) within [ATP$_2$⊂**1**-H$_6$]$^{2+}$ and [ADP$_2$⊂**1**-H$_6$]$^{4+}$ as obtained from 640 ns REMD simulations (298 – 370 K); for clarity, the illustrations are only showing one nucleotide per host. (B) Single crystal X-ray structure of [ATP$_2$⊂**1**-H$_6$]$^{2+}$ with host-guest N–H---O HBs (I-V; 2.696-3.20 Å) and π–π stacking (VI, <3.6 Å) interactions.

and rearrangements. For [ATP$_2$⊂**1**–H$_6$]$^{2+}$ placed in a box of water molecules, each triphosphate tail from the guests occupies one pocket of the host. However, adenine bases would spend 55% of the

simulation time within π–π stacking distance of a benzene arm from the host and 75% of that time associating with a benzene from the neighboring pocket occupied by the phosphate from another ATP (Figure 4A). On the other side, $[ADP_2\subset\mathbf{1}\text{–}H_6]^{4+}$ assumes a geometry that, for most of the simulation time (58%, Figure 4A), has each of adenine bases π–π stack with benzene arms from the chamber holding its phosphate moiety. The computational results are thus in support of our experimental observations disclosing the synergy of charged hydrogen bonding and π–π stacking for establishing the allosteric encapsulation of nucleotides. Finally, X-ray structure of $[ATP_2\subset\mathbf{1}\text{–}H_6]^{2+}$ (Figure 4B) corroborates the spectroscopic and computational findings with two ATP molecules populating two cavities of **1** in the similar manner with the notion that packing in solid state could have some effect on the mode of binding. The phosphate groups form up to five HB contacts with ammoniums (I-III) and amides (IV-V) while each adenine base π–π stacks with benzene groups from the neighbouring pockets (VIII). The fact one ATP guest in Figure 4B forms an additional HB with the host along with its more extensive π–π contacts (i.e. a greater surface overlap) could explain the negative allostery (α = 0.6, Table 1) observed for the consecutive binding events.

In conclusion, we developed a synthetic method for obtaining dual-cavity host of type **1**. This novel abiotic receptor traps two molecules of ATP in water by a synergistic action of hydrogen bonding and π–π stacking contacts. With facile access to **1** and, perhaps, its derivatives possessing other aromatics as side walls, this work sets the stage for exploring the preparation of novel and allosteric chemosensors, colorimetric reagents and sequesters of nucleotides.

Conflicts of interest

There are no conflicts to declare.

Notes and references

1 (a) B. Chance, H. Lees and J. R. Postgate, *Nature*, 1972, **238**, 330-331; (b) A. Mishra, S. Dhiman and S. J. George, *Angew. Chem., Int. Ed.*, 2021, **60**, 2740-2756.
2 J. R. Knowles, *Annu. Rev. Biochem.*, 1980, **49**, 877-919.
3 A. E. Hargrove, S. Nieto, T. Zhang, J. L. Sessler and E. V. Anslyn, *Chem. Rev.*, 2011, **111**, 6603-6782.
4 (a) C. Bazzicalupi, S. Biagini, A. Bencini, E. Faggi, C. Giorgi, I. Matera and B. Valtancoli, *Chem. Commun.*, 2006, 4087-4089; (b) Z. Xu, N. R. Song, J. H. Moon, J. Y. Lee and J. Yoon, *Org. Biomol. Chem.*, 2011, **9**, 8340-8345; (c) P. P. Neelakandan, M. Hariharan and D. Ramaiah, *Org. Lett.*, 2005, **7**, 5765-5768; (d) D. Cheng, Y. Li, J. Wang, Y. Sun, L. Jin, C. Li and Y. Lu, *Chem. Commun.*, 2015, **51**, 8544-8546.
5 (a) P. Srivastava, S. S. Razi, R. Ali, S. Srivastav, S. Patnaik, S. Srikrishna and A. Misra, *Biosens. Bioelectron.*, 2015, **69**, 179-185; (b) D. Maity, M. Li, M. Ehlers and C. Schmuck, *Chem. Commun.*, 2017, **53**, 208-211.
6 (a) C. Chen, Y. Chen, X. Dai, J. Li, S. Jia, S. Wang and Y. Liu, *Chem. Commun.*, 2021, **57**, 2812-2815; (b) G. Yu, J. Zhou, J. Shen, G. Tang and F. Huang, *Chem. Sci.*, 2016, **7**, 4073-4078.
7 P. P. Neelakandan, M. Hariharan and D. Ramaiah, *J. Am. Chem. Soc.*, 2006, **128**, 11334-11335.
8 M. M. Gottesman, T. Fojo and S. E. Bates, *Nat. Rev. Cancer*, 2002, **2**, 48-58.
9 P. P. Neelakandan, P. C. Nandajan, B. Subymol and D. Ramaiah, *Org. Biomol. Chem.*, 2011, **9**, 1021-1029.
10 W. Wang, T. J. Finnegan, Z. Lei, X. Zhu, C. E. Moore, K. Shi and J. D. Badjic, *Chem. Commun.*, 2020, **56**, 1271-1274.
11 J. A. Riddle, X. Jiang, J. Huffman and D. Lee, *Angew. Chem., Int. Ed.*, 2007, **46**, 7019-7022.
12 S. Shinkai, M. Ikeda, A. Sugasaki and M. Takeuchi, *Acc. Chem. Res.*, 2001, **34**, 494-503.
13 G. Hennrich and E. V. Anslyn, *Chem. Eur. J.*, 2002, **8**, 2218-2224.
14 (a) A. P. Bisson, V. M. Lynch, M.-K. C. Monahan and E. V. Anslyn, *Angew. Chem., Int. Ed. Engl.*, 1997, **36**, 2340-2342; (b) N. De Rycke, J. Marrot, F. Couty and O. R. P. David, *Tetrahedron Lett.*, 2010, **51**, 6521-6525; (c) R. L. Greenaway, V. Santolini, F. T. Szczypinski, M. J. Bennison, M. A. Little, A. Marsh, K. E. Jelfs and A. I. Cooper, *Chem. Eur. J.*, 2020, **26**, 3718-3722.
15 F. Wang, E. Sikma, Z. Duan, T. Sarma, C. Lei, Z. Zhang, S. M. Humphrey and J. L. Sessler, *Chem. Commun.*, 2019, **55**, 6185-6188.
16 (a) R. A. Tromans, T. S. Carter, L. Chabanne, M. P. Crump, H. Li, J. V. Matlock, M. G. Orchard and A. P. Davis, *Nat. Chem.*, 2019, **11**, 52-56; (b) O. Francesconi, A. Ienco, G. Moneti, C. Nativi and S. Roelens, *Angew. Chem., Int. Ed.*, 2006, **45**, 6693-6696.
17 (a) J. H. Oh, J. H. Kim, D. S. Kim, H. J. Han, V. M. Lynch, J. L. Sessler and S. K. Kim, *Org. Lett.*, 2019, **21**, 4336-4339; (b) M. Arunachalam, I. Ravikumar and P. Ghosh, *J. Org. Chem.*, 2008, **73**, 9144-9147; (c) J. Romanski and P. Piatek, *J. Org. Chem.*, 2013, **78**, 4341-4347; (d) H. J. Han, J. H. Oh, J. L. Sessler and S. K. Kim, *Chem. Commun.*, 2019, **55**, 10876-10879.
18 R. A. S. Vasdev, D. Preston and J. D. Crowley, *Chem. Asian J.*, 2017, **12**, 2513-2523.
19 H. Xie, T. J. Finnegan, V. W. Liyana Gunawardana, R. Z. Pavlovic, C. E. Moore and J. D. Badjic, *J. Am. Chem. Soc.*, 2021, **143**, 3874-3880.
20 (a) M. E. Belowich and J. F. Stoddart, *Chem. Soc. Rev.*, 2012, **41**, 2003-2024; (b) Z. Yang, C. Yu, J. Ding, L. Chen, H. Liu, Y. Ye, P. Li, J. Chen, K. J. Wu, Q.-Y. Zhu, Y.-Q. Zhao, X. Liu, X. Zhuang and S. Zhang, *Nat. Commun.*, 2021, **12**, 6124.
21 H. Xie, V. W. L. Gunawardana, T. J. Finnegan, W. Xie and J. D. Badjic, *Angew. Chem., Int. Ed.*, **2022**, Ahead of Print.
22 S. Chen, M. Yamasaki, S. Polen, J. Gallucci, C. M. Hadad and J. D. Badjic, *J. Am. Chem. Soc.*, 2015, **137**, 12276-12281.
23 Q. P. B. Nguyen, T. N. Le and T. H. Kim, *Bull. Kor. Chem. Soc.*, 2009, **30**, 1743-1748.
24 P. T. Glink, A. I. Oliva, J. F. Stoddart, A. J. P. White and D. J. Williams, *Angew. Chem., Int. Ed.*, 2001, **40**, 1870-1875.
25 J. D. Badjic, S. Stojanovic and Y. Ruan, *Adv. Phys. Org. Chem.*, 2011, **45**, 1-37.
26 S. Chakraborty, M. Arunachalam, P. Bose and P. Ghosh, *Cryst. Growth Des.*, 2013, **13**, 3208-3215.
27 N. A. Corfu and H. Sigel, *Eur. J. Biochem.*, 1991, **199**, 659-669.
28 Brynn Hibbert and P. Thordarson, *Chem. Commun.*, 2016, **52**, 12792-12805.
29 P. Thordarson, *Chemical Society Reviews*, 2011, **40**, 5922-5923.
30 R. A. Alberty, R. M. Smith and R. M. Bock, *J Biol Chem*, 1951, **193**, 425-434.
31 P. I. Kitov and D. R. Bundle, *J. Am. Chem. Soc.*, 2003, **125**, 16271-16284.
32 R. Qi, G. Wei, B. Ma and R. Nussinov, *Methods Mol. Biol.* 2018, **1777**, 101-119.